

# Conflict Forecasting via Conformal Prediction for Markov Processes

Aditya Basarkar<sup>1</sup>, Emmett B. Kendall<sup>2</sup>, David Randahl<sup>3</sup>,  
Jonathan P. Williams<sup>1</sup>, and Gudmund H. Hermansen<sup>4</sup>

<sup>1</sup>Department of Statistics, North Carolina State University

<sup>2</sup>Department of Mathematical Sciences, The University of Texas at Dallas

<sup>3</sup>Department of War Studies, Swedish Defense University

<sup>4</sup>Department of Mathematics, University of Oslo

## Abstract

Whether or not a country is at war, or experiencing escalating or deescalating levels of conflict, has massive ramifications on a country's national and foreign policy. Given a country's history of conflict, or lack thereof, future predictions about the war-status of a country are valuable information. In this paper, we present the use of conformal prediction on temporally-dependent data to obtain prediction sets of possible future conflict state-sequences. More specifically, we compare the results of conformal prediction to a likelihood-based prediction strategy when the data are assumed to come from a discrete-state Markov process. A point-prediction may not supply sufficient information because the penalty for a wrong prediction is extreme, and so we consider a machine learning alternative that gives valid uncertainty quantification and is robust to model misspecification. In the data analysis, we present real forecasts of conflict dynamics across multiple countries. Lastly, we comment on the possible limitations of existing approaches for applying conformal prediction to Markovian data, where the exchangeability assumption is violated.

*Keywords:* conflict dynamics, multistate model, non-exchangeable data, state-space model, time series

# 1 Motivation

The last decade has seen a surge of interest in forecasting conflict dynamics within peace and conflict research. Driven by increased access to fine-grained data and advances in machine learning and computing, several large-scale forecasting projects have emerged targeting armed conflict and related phenomena such as coups, electoral violence, and regime change [see for instance Hegre et al., 2019, 2021, Randahl et al., 2025, Ward and Beger, 2017, Morgan et al., 2019]. Early efforts focused on point predictions, but there is growing recognition that uncertainty quantification is equally critical: incorrect predictions carry severe consequences, and decision-makers require not just a single forecast but a calibrated sense of the range of plausible outcomes [Hegre et al., 2025, Randahl et al., 2026]. This has motivated a shift toward probabilistic forecasting methods and prediction intervals/sets.

Among the models that have shown promise for conflict dynamics are Markov models, which represent the evolution of a conflict system as a sequence of states transitioning over time [Randahl and Vegelius, 2022, Williams et al., 2024]. Combined with estimated conditional distributions of fatality counts given the current state, these models can generate forecasts of future conflict trajectories [Randahl and Vegelius, 2024, Hegre et al., 2025]. However, their uncertainty estimates are sensitive to model misspecification, a serious concern given the difficulty of correctly characterizing conflict processes.

Conformal prediction (CP) offers a principled alternative. By requiring only an exchangeability assumption rather than a correctly specified model, CP produces prediction sets with finite-sample marginal coverage guarantees. In this paper, we explore applying CP to discrete-state Markov processes to generate valid prediction sets for future conflict state-sequences, and we compare its performance against likelihood-based approaches. A key challenge we address is that Markov processes, by definition, violate the standard exchangeability assumption underlying conformal methods, and we discuss the implications and limitations of existing approaches for handling their temporal dependence.

The remainder of this article is structured as follows. Section 2 provides background on the statistical strategies being employed, followed by Section 3 which provides an in-depth description of our methodology and algorithm. Next, Section 4 presents the results of both the simulation study and real data analysis. Then, Section 5 offers insight into the potential limitations of the approach being presented, and lastly, Section 6 shares final remarks and conclusions.

## 2 Background

CP offers a robust approach to construct prediction sets that obtain valid coverage for exchangeable data [see Shafer and Vovk, 2008, Vovk et al., 2022, for more on CP]. The development of CP has proven to be a very powerful statistical strategy given its finite-sample validity guarantees. Its utility is elucidated by the breadth of fields applying CP methods. These examples include real estate [Hjort et al., 2024, 2025], autonomous cars [Bang et al., 2024], spatial statistics [Mao et al., 2024], networks [Dashevskiy and Luo, 2008, Luo et al., 2023], and more. However, CP relies on the assumption that the data are exchangeable, which in many applications, need not be the case. Hence, much of the aforementioned research, as well as what is presented in this article, discusses how to reformulate the CP algorithm to maintain its statistical guarantees when the data are

not inherently exchangeable. The focus for this work is on time series data, particularly Markov processes, where sequential observations are temporally dependent.

Methodological developments in CP for time series data has a well-studied literature [e.g., Xu and Xie, 2021, 2023, Zheng and Proutiere, 2024, Dua et al., 2025, Neglia et al., 2025]. Many of these approaches focus on developing provably valid, or approximately valid, methods for data that exhibit dependencies which violate the exchangeability assumption. One example is the development of adaptive CP, which calibrates the guaranteed confidence level in an online setting to account for on-going distributional changes in the data [Gibbs and Candes, 2021, Zaffran et al., 2022, Su et al., 2024]. Other approaches seek to re-frame *where* the notion of exchangeability is applied.

This latter approach can be split into two different frameworks, specifically for handling discrete-state Markov processes. The first idea is to treat each state-sequence as an individual observation, and then multiple observations of these state-sequences are assumed to be independent and thus exchangeable [Cherubin and Nourtdinov, 2016, Stankeviciute et al., 2021]. However, instead of relying on multiple realizations of independent state-sequences, the second idea leverages properties of Markov processes and permutation-groups to arrive at a notion of partial exchangeability for a *single* state-sequence [Chernozhukov et al., 2018, 2021, Nettasinghe et al., 2023] (more detail in Section 3.1). In either case, the output of the CP algorithm remains a prediction set of forecasted state-sequences.

Further research has been conducted to extend CP to doubly stochastic processes, like via CP for hidden Markov models (HMMs) [Cherubin and Nourtdinov, 2016, Nettasinghe et al., 2023, Su et al., 2024]. For the purposes of our work, particular focus is afforded to the methodology developed in Nettasinghe et al. [2023]. In particular, we apply the algorithmic procedure developed in Nettasinghe et al. [2023] to the case of discrete-state Markov models, rather than discrete-state HMMs.

## 3 Methodology

Let  $\{X_t\}_{t=1}^T$  denote a discrete-state Markov process observed over  $T > 0$  time points, where  $X_t \in \mathcal{X} = \{1, 2, \dots, m\}$ ,  $m \in \mathbb{Z}^+$ . We refer to  $\{X_t\}_{t=1}^T$  as the *calibration* sequence/data. The ultimate goal for this work is to forecast state-sequences  $T_1 > 0$  time points into the future. Rather than constructing a point-prediction (i.e., one future state-sequence of length  $T_1$ ), our goal instead is to construct a prediction set, for any level  $1 - \alpha \in (0, 1)$ , of state-sequences, say  $\mathcal{C}_{1-\alpha}$ , that guarantees the true underlying state-sequence is an element of the set with probability at least  $1 - \alpha$ . We present two approaches to constructing prediction sets: (1) CP in Section 3.1, and (2) likelihood-based prediction in Section 3.2, with more attention afforded to the former.

### 3.1 Conformal Prediction

As noted before, the methodology described here is a reflection of the work of Nettasinghe et al. [2023]; however, rather than considering doubly-stochastic processes (like with HMMs), we take a simpler approach making predictions for a single observed time series. Applying the notion of exchangeability to the individual observations of a Markov process is not feasible given the inherent probabilistic dependencies over time. Consequently, we can leverage the idea of *partial exchangeability* which applies the exchangeability principle, not

to each observed time point, but to the entire state-sequence. In particular, given two realized state-sequences of a discrete-time, discrete-state Markov process (of order 1)  $\{x_t\}_{t=1}^T$  and  $\{x'_t\}_{t=1}^T$ , if (1)  $x_1 = x'_1$ , and (2) the number of observed transitions between states is the same in  $\{x_t\}_{t=1}^T$  and  $\{x'_t\}_{t=1}^T$ , then these sequences must be partially exchangeable in the sense that  $\mathbb{P}(\{X_t = x_t\}_{t=1}^T) = \mathbb{P}(\{X_t = x'_t\}_{t=1}^T)$  [Nettasinghe et al., 2023].

---

**Algorithm 1** CP algorithm for discrete-state Markov process, adapted from Nettasinghe et al. [2023]

---

**Input:** Calibration data  $\{X_t\}_{t=1}^T$ , miscoverage  $\alpha \in (0, 1)$ , maximum number of permutations  $n$

**Output:** Prediction set  $\mathcal{C}_{1-\alpha} \subseteq \mathcal{X}^{T_1}$ , where  $\mathcal{X}^{T_1}$  is the set of all possible state-sequences of length  $T_1$

**for**  $\mathbf{x} = (x_{T+1}, \dots, x_{T+T_1}) \in \mathcal{X}^{T_1}$  **do**

1. Set  $X_{T+1} = x_{T+1}, \dots, X_{T+T_1} = x_{T+T_1}$
2. Using  $\{X_t\}_{t=1}^{T+T_1}$ , estimate the transition probability matrix ( $\mathbf{P}$ ) by

$$[\hat{\mathbf{P}}]_{i,j} = \frac{\sum_{t=1}^{T+T_1-1} \mathbf{1}(X_t = i \wedge X_{t+1} = j)}{\sum_{t=1}^{T+T_1-1} \mathbf{1}(X_t = i)}$$

3. Determine the set of permutable  $i$ -blocks,  $\mathcal{I} = \{I_1, \dots, I_D\}$ , given  $X_{T+T_1} = x_{T+T_1} = i$ .
4. Let  $\mathcal{P}$  be the permutation group of  $\mathcal{I}$  where each  $\rho \in \mathcal{P}$  results in  $\{I_1^{(\rho)}, \dots, I_D^{(\rho)}\}$ . Then

$$\{X_t^{(\rho)}\}_{t=1}^{T+T_1} = \begin{cases} \{I_1^{(\rho)}, \dots, I_D^{(\rho)}, I_{D+1}\}, & X_1 = i \\ \{I_0, I_1^{(\rho)}, \dots, I_D^{(\rho)}, I_{D+1}\}, & \text{otherwise} \end{cases}$$

Let  $\mathbf{I}$  denote the original, un-permuted sequence  $\{X_t\}_{t=1}^{T+T_1}$  (i.e., “identity permutation”)

5. For computational purposes

$$\Pi := \begin{cases} \mathcal{P}, & \text{if } |\mathcal{P}| \leq n \\ \text{a random sample without replacement of size } n \text{ from } \mathcal{P}, & \text{if } |\mathcal{P}| > n \end{cases}$$

**for**  $\pi \in \Pi$  **do**

Calculate the non-conformity score  $S(\pi)$

$$S(\pi) = 1 - \frac{\sum_{j=1}^{T_1} \mathbb{P}_{\hat{\mathbf{P}}}(X_{T+j}^{(\pi)} | X_T^{(\pi)})}{T_1}$$

**end for**

6. Calculate the p-value

$$\hat{q}(\mathbf{x}) = \frac{\sum_{\pi \in \Pi} \mathbf{1}\{S(\pi) > S(\mathbf{I})\} + u \cdot \mathbf{1}\{S(\pi) = S(\mathbf{I})\}}{|\Pi|},$$

where  $\mathbf{I}$  is the identity permutation (refer to step 4), and  $u \sim \text{Uniform}[0, 1]$ .

**end for**

**return**  $\mathcal{C}_{1-\alpha} = \{\mathbf{x} \in \mathcal{X}^{T_1} : \hat{q}(\mathbf{x}) > \alpha\}$

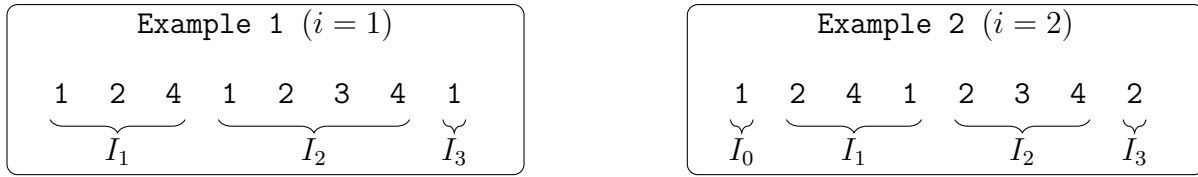
---

Algorithm 1 outlines the CP routine for constructing  $(1 - \alpha)$ -level prediction sets for the forecasted state-sequences of length  $T_1$ . The following is a detailed overview of the mechanics of the algorithm, specifically focusing on how the partial exchangeability assumption manifests. Based on the work of Chernozhukov et al. [2018, 2021], the idea presented in Nettasinghe et al. [2023] is to test if a proposed sequence  $(x_{T+1}, \dots, x_{T+T_1})$  belongs in the prediction set based on the exchangeability of permutable segments of the sequence,  $\{X_t\}_{t=1}^{T+T_1}$ , where it is assumed  $X_{T+1} = x_{T+1}, \dots, X_{T+T_1} = x_{T+T_1}$  (refer to  $\{X_t\}_{t=1}^{T+T_1}$  as the *augmented* sequence). In particular, the authors break the augmented sequence into what they term “ $i$ -blocks,” which are sequences of state-observations that begin with  $i \in \mathcal{X}$

and include no further  $i$ 's. For the purposes of Algorithm 1, the choice of  $i$  is completely determined by the proposed value for  $X_{T+T_1}$ . With these  $i$ -blocks, the augmented sequence  $\{X_t\}_{t=1}^{T+T_1}$  can be represented as

$$\{X_t\}_{t=1}^{T+T_1} = \begin{cases} \{I_1, \dots, I_D, I_{D+1}\}, & \text{if } X_1 = i \\ \{I_0, I_1, \dots, I_D, I_{D+1}\}, & \text{otherwise} \end{cases} \quad (1)$$

where  $I_d$ ,  $d \in \{1, 2, \dots, D\}$ , denotes a single permutable  $i$ -block and  $D$  is the total number of  $i$ -blocks. Note that  $I_0$  and  $I_{D+1}$  are *not* considered  $i$ -blocks because these cannot be permuted without changing the counts of state transitions of the original, un-permuted sequence  $\{X_t\}_{t=1}^{T+T_1}$  (i.e., the *identity permutation*). Define  $\mathcal{I} := \{I_1, \dots, I_D\}$  to be the set of all permutable  $i$ -blocks. In order to better understand the two cases in (1), consider the two following simple examples of breaking a state-sequence into  $i$ -blocks where  $\mathcal{X} = \{1, 2, 3, 4\}$ , and the only difference is the state at the last time point, namely  $X_{T+T_1} = x_{T+T_1} = i$ .



In both cases,  $D = 2$  and  $\mathcal{I} = \{I_1, I_2\}$ . For Example 1, there exists two partially exchangeable sequences, namely  $\{I_1, I_2, I_3\}$  (the identity permutation) and  $\{I_2, I_1, I_3\}$ ; for Example 2, the partially exchangeable sequences are  $\{I_0, I_1, I_2, I_3\}$  (the identity permutation) and  $\{I_0, I_2, I_1, I_3\}$ . In each example, no matter how we permute  $I_1$  and  $I_2$ , the resulting state-sequence will have the same number of state transitions as the initial, un-permuted augmented sequence. Provided this intuition for partial exchangeability, we now have the architecture to obtain valid,  $(1 - \alpha)$ -level prediction sets for state-sequences  $T_1$  time points into the future (see Nettasinghe et al. [2023] for proof of validity).

### 3.2 Likelihood-Based Prediction

An alternative approach to CP is to simply fit a Markov model to the observed state-sequences in the calibration data and obtain likelihood-based prediction sets for forecasted state-sequences of length  $T_1$ . This approach serves as a baseline comparison to the prediction sets obtained using CP. However, unlike CP, this method does not offer finite-sample guarantees that are independent of model correctness (i.e., not robust to model-misspecification).

The likelihood-based prediction sets for individual state-sequences are constructed as follows. Using the calibration data,  $\{X_t\}_{t=1}^T$ , we first fit a Markov model by estimating the transition probability matrix  $\hat{\mathbf{P}}$  (same as step 2 of Algorithm 1). Then, if  $\mathcal{X}^{T_1} = \{\mathbf{x}^1, \dots, \mathbf{x}^J\}$  denotes the set of all possible state-sequences of length  $T_1$  ( $J = |\mathcal{X}^{T_1}|$ ), we find

$$\begin{aligned} \mathbb{P}(\mathbf{X}_{T+1}^{T+T_1} = \mathbf{x}^j \mid X_T = x_T) &:= \mathbb{P}(X_{T+1} = x_{T+1}^j, \dots, X_{T+T_1} = x_{T+T_1}^j \mid X_T = x_T) \\ &= [\hat{\mathbf{P}}]_{x_T, x_{T+1}^j} \cdot \prod_{t=2}^{T_1} [\hat{\mathbf{P}}]_{x_{T+t-1}^j, x_{T+t}^j} \end{aligned} \quad (2)$$

for all  $j \in \{1, 2, \dots, J\}$ , where  $[\cdot]_{k,l}$  denotes the  $k^{\text{th}}$  row and  $l^{\text{th}}$  column of a matrix argument. Next, let  $\mathbf{x}^{(1)}, \mathbf{x}^{(2)}, \dots, \mathbf{x}^{(J)} \in \mathcal{X}^{T_1}$  denote the ordered elements (greatest to least) of  $\mathcal{X}^{T_1}$  based on the probability mass computed in (2). The likelihood-based prediction set at level  $(1 - \alpha)$  is taken to be the highest probability mass set:

$$\mathcal{C}_{1-\alpha}^{\text{like}} := \{\mathbf{x}^{(1)}, \dots, \mathbf{x}^{(K)}\}, \quad (3)$$

where

$$K = \min \left\{ k \in \{1, 2, \dots, J\} \left| \sum_{j=1}^k \mathbb{P}(\mathbf{X}_{T+1}^{T+T_1} = \mathbf{x}^{(j)} \mid X_T = x_T) \geq 1 - \alpha \right. \right\}.$$

In the case of ties where, say,  $\mathbb{P}(\mathbf{X}_{T+1}^{T+T_1} = \mathbf{x}^\ell \mid X_T = x_T) = \mathbb{P}(\mathbf{X}_{T+1}^{T+T_1} = \mathbf{x}^j \mid X_T = x_T)$  for  $\ell, j \in \{1, \dots, J\}$ ,  $\ell \neq j$ , the ordering of  $\mathbf{x}^\ell$  and  $\mathbf{x}^j$  is determined uniformly at random. This handling of ties is analogous to sampling  $u \sim \text{Uniform}[0, 1]$  in step 6 of Algorithm 1 for CP. It is important to note that alternative approaches exist for constructing these likelihood-based prediction sets (see Appendix Section 7); our motivation for choosing this highest-density-region approach is that it guarantees the minimal cardinality over all prediction sets having probability mass of at least  $1 - \alpha$ .

## 4 Experiments and Evaluation

### 4.1 Data Description and Cleaning

The data for this work comes from Uppsala Conflict Data Programme (UCDP), which tracks fatalities from organized violence across the world [Davies et al., 2025]. In particular, we utilize the UCDP Georeferenced Event Dataset (GED) Global, and aggregate the data to the country-month level [Sundberg and Melander, 2013]. Each observation corresponds to the number of fatalities from state-based conflict observed for a given country in a given month. In total, we utilize data from 191 countries from January of 1990 until July of 2025. Building on the Markov structure proposed by Randahl and Vegelius [2022, 2024], we deterministically assign state-labels to these counts in order to categorize the type of conflict-state that a given country is in at any given month. We will consider four states: (1) peacetime, (2) escalation, (3) war, and (4) deescalation. Let  $Y_{i,t}$  denote the number of casualties observed for country  $i$ ,  $i \in \{1, 2, \dots, 191\}$ , at month  $t$ . The assigned state-label,  $X_{i,t}$ , is determined by the following rules:

$$X_{i,t} = \begin{cases} 1, & \text{if } Y_{i,t-1} = Y_{i,t} = 0 \text{ for } t > 1, \text{ or } Y_{i,t} = 0 \text{ for } t = 1 \\ 2, & \text{if } Y_{i,t-1} = 0 \text{ and } Y_{i,t} > 0 \text{ for } t > 1 \\ 3, & \text{if } Y_{i,t-1} > 0 \text{ and } Y_{i,t} > 0 \text{ for } t > 1, \text{ or } Y_{i,t} > 0 \text{ for } t = 1 \\ 4, & \text{if } Y_{i,t-1} > 0 \text{ and } Y_{i,t} = 0 \text{ for } t > 1. \end{cases}$$

Note that the only data used in the analysis are these assigned state-labels over time. From these state-labels, Figure 1 illustrates the allowable state transitions and corresponding adjacency matrix.

Next, we clean the data according to the following rule: the countries kept in the analysis must have at least *five* observations that are not in peacetime (i.e., at least five

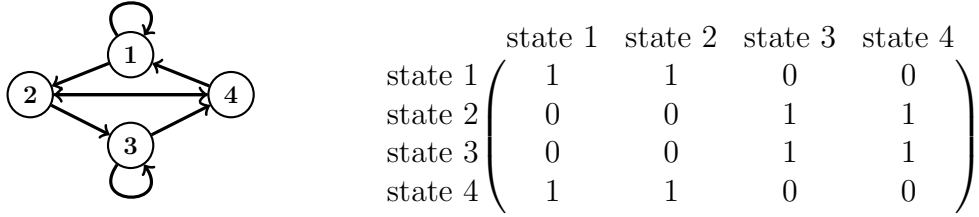


Figure 1: All allowable state transitions between the four conflict-states (left), and the corresponding adjacency matrix (right), where states 1, 2, 3, and 4 correspond to peacetime, escalation, war, and deescalation, respectively.

observations of states 2, 3, and/or 4), and the proportion of instances of peacetime (state 1) does not exceed 0.99 for a given country. In summary, the goal of this rule is to exclude countries that have the same state observed across all (or almost all) time points, and in these data, we find this occurs often with countries in peacetime (state 1). The only exception to this is Ukraine, which remains in war (state 3) for all observations, thus we also exclude it from our analysis. Additional insight which motivates this data-cleaning procedure is found in Section 5. After cleaning the data, we are left with 86 countries in our analysis.

## 4.2 Simulation Study

In order to evaluate the methods discussed in Section 3, we present a Monte Carlo simulation study where the true data generating mechanism is known. The data are simulated as a Markov process where the true transition probability matrix,  $\mathbf{P}$ , and initial state distribution,  $\boldsymbol{\pi}$ , are given as

$$\mathbf{P} = \begin{pmatrix} 0.895 & 0.105 & 0 & 0 \\ 0 & 0 & 0.500 & 0.500 \\ 0 & 0 & 0.722 & 0.278 \\ 0.653 & 0.347 & 0 & 0 \end{pmatrix}, \quad \boldsymbol{\pi} = (0.25 \quad 0.25 \quad 0.25 \quad 0.25). \quad (4)$$

These true values are informed by the cleaned, real data. In particular, using the estimator from step 2 of Algorithm 1, we compute an estimated transition probability matrix for each country, and then average (component-wise) the estimated transition probability matrices to determine the values in  $\mathbf{P}$ . For the true initial state probabilities,  $\boldsymbol{\pi}$ , we assign equal probability to starting in any one of the four states.

We can evaluate the CP and likelihood-based approaches by comparing both their reliability curves as well as the composition of their prediction sets for prespecified confidence levels and forecast lengths. For each simulation,  $T = 200$  is the length of the calibration sequence. Next, let  $T_1 \in \{1, 2, \dots, 6\}$  denote the test length of the forecasted state-sequence. Then, in order to compare the empirical coverages of the CP and likelihood-based approaches for each  $T_1$ , we run the simulation for a range of confidence levels, namely for  $1 - \alpha \in \{0.50, 0.55, \dots, 1.00\}$ . For each combination of  $T_1$  and  $1 - \alpha$ , we simulate 500 state-sequences of length  $T + T_1$  according to the Markov process defined by (4). The CP and likelihood-based prediction sets are constructed using the first  $T$  time points (the calibration data), and then for each of the 500 simulations, we can determine whether or not the prediction sets [for the last  $T_1$  time points] contain the true forecasted state-sequence.

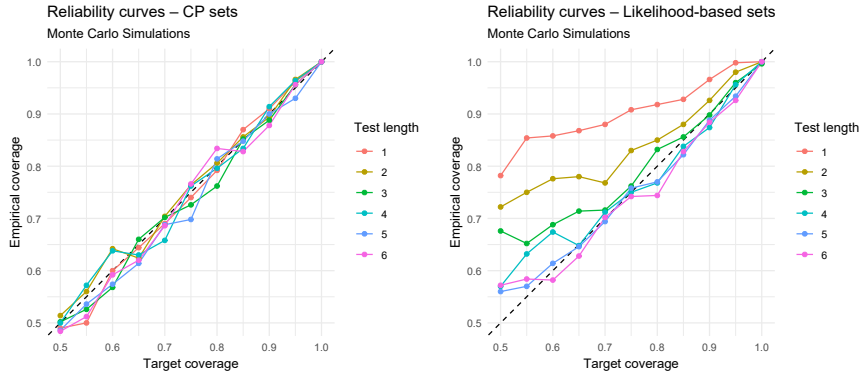


Figure 2: Reliability curves illustrating the relationship between the empirical coverage and the target coverage for both the CP approach (left) and likelihood-based prediction approach (right) for the simulated data.

The empirical coverage is then determined as the proportion of the 500 prediction sets that contain the true forecasted state-sequence.

Figure 2 presents the reliability curves for the conformal and likelihood-based predictions. We see that the CP approach remains well calibrated for all confidence levels and test lengths, consistent with the results in Nettasinghe et al. [2023]. In the case of the likelihood-based approach, however, we see that as both the test length and confidence level decrease, the prediction sets tend to *over-cover*. Insight into the over-coverage exhibited by the likelihood-based approach is provided in Section 4.2.1.

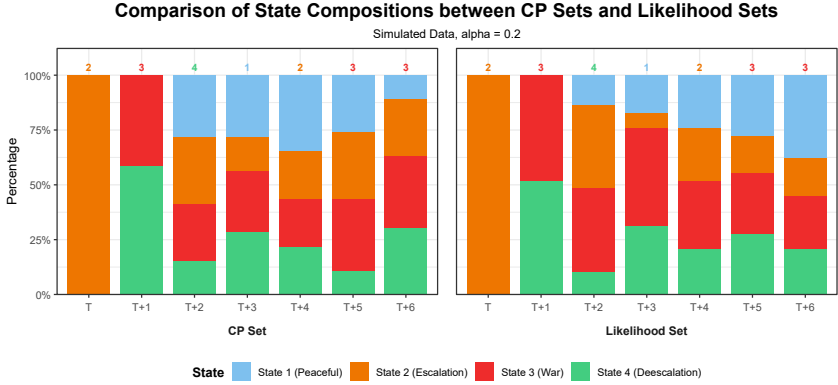


Figure 3: Visualization of the prediction sets for a single simulated state-sequence resulting from the conformal (left) and likelihood-based (right) prediction approaches. Note that the state at time  $T$  (i.e.,  $X_T$ ) is *not* being forecasted; however, the realized value of  $X_T$  is being plotted because the possible forecasted state-sequences  $(X_{T+1}, \dots, X_{T+T_1})$  depend on  $X_T$  by way of the Markov assumption.

Next, Figure 3 is a visualization of the prediction sets for a single simulated state-sequence where  $T = 200$ ,  $T_1 = 6$ , and  $1 - \alpha = 0.80$ , using both the conformal and likelihood-based methods. Figure 3 has the following interpretation: taking all state-sequences in the prediction set, the proportion of each state at each time point  $(T + 1, T + 2, \dots, T + T_1)$  is represented by the proportion of each corresponding color in each vertical bar. In this case, the true forecasted state for each future time point is denoted by the colored numeral above each vertical bar. The results in Figure 3 illustrate an important difference between the CP

and likelihood-based approaches. We see that as the test length,  $T_1$ , increases, the composition of the prediction sets produced from the likelihood-based approach converges to its stationary distribution; however, the CP approach produces a more diverse set of forecasted state-sequences, with a difference more clearly pronounced for the later time points (e.g.,  $T + 6$ ). For example, given  $X_T = 2$  in Figure 3 and given the true model in (4), we can estimate the stationary distribution  $P(X_{T+\infty} | X_T = 2) = (0.6206, 0.0999, 0.1796, 0.0999)$ ; this conditional probability mass is close to the composition of predicted states at time  $T + 6$  for the likelihood-based approach.

Lastly, Table 1 presents the differences in the cardinality of the prediction sets between the conformal and likelihood-based prediction algorithms. On average, the likelihood-based prediction sets contain fewer predicted state-sequences than the CP sets (with exception to  $T_1 = 1$  and target coverage 0.55). As mentioned in Section 3.2, the likelihood-based prediction sets are constructed as efficiently as possible given that the model is correctly specified in the simulation study, in the sense of minimizing the number of forecasted state-sequences while guaranteeing a cumulative probability mass of at least  $1 - \alpha$ . Although the greater cardinality suggests that CP is less efficient than the likelihood-based approach, Figure 2 indicates that the likelihood-based approach tends to over-cover due to fewer sequences accounting for most of the probability mass.

	Target Coverage									
	0.55		0.65		0.75		0.85		0.95	
	CP	Like.	CP	Like.	CP	Like.	CP	Like.	CP	Like.
$(T_1 = 1)$	0.86	1.04	1.23	1.19	1.51	1.36	1.61	1.36	1.87	2.00
$(T_1 = 2)$	1.47	1.18	1.84	1.50	2.26	1.81	2.67	2.32	3.63	3.45
$(T_1 = 3)$	2.68	1.41	3.06	1.69	3.97	2.74	4.81	3.91	6.76	6.15
$(T_1 = 4)$	3.76	2.15	5.09	2.61	6.74	4.10	9.58	6.46	13.46	10.75
$(T_1 = 5)$	6.12	2.57	9.07	4.05	13.44	6.82	18.37	10.34	25.79	18.78
$(T_1 = 6)$	11.28	4.14	17.16	7.16	24.50	10.35	35.51	18.23	50.19	33.87

Table 1: Comparison of the cardinality of prediction sets using CP and likelihood-based prediction (“Like.”) for the simulation over different prediction lengths,  $T_1$ , and target coverage levels. The results are averaged over 100 simulations.

#### 4.2.1 Insight into Over-Coverage for Likelihood-Based Approach

In order to gain intuition for the over-coverage observed in the likelihood-based approach in Figure 2, let us focus on the simplest case where  $T_1 = 1$  and the target coverage is  $1 - \alpha = 0.50$ . Recall how the likelihood-based prediction set,  $\mathcal{C}_{1-\alpha}^{\text{like}}$ , is defined from Section 3.2. Given the state at time  $T$  ( $X_T = x_T$ ) and  $T_1 = 1$ , we know that  $\mathcal{C}_{1-\alpha}^{\text{like}}$  will comprise of either only one or two states. This certainty comes from the fact that in each row of the adjacency matrix in Figure 1, there only ever exists two non-zero entries. From the true model in (4), the maximum transition probability in each row of  $\mathbf{P}$  is at least 0.50, and recall we are considering the case when the target coverage is  $1 - \alpha = 0.50$ . Note that while the true  $\mathbf{P}$  is never used in the construction of  $\mathcal{C}_{1-\alpha}^{\text{like}}$ , we know  $\hat{\mathbf{P}} \approx \mathbf{P}$  on average because  $T = 200$  is sufficiently large. Given this setup, we know that for a target coverage  $1 - \alpha = 0.50$ , the average cardinality of  $\mathcal{C}_{1-\alpha}^{\text{like}}$  is one. This is because the forecasted

state-sequence of length  $T_1 = 1$  in  $\mathcal{C}_{1-\alpha}^{\text{like}}$  is simply the state corresponding to the maximum transition probability in the  $x_T$  row of  $\hat{\mathbf{P}}$  which, on average, is at least  $1 - \alpha = 0.50$ .

While the empirical coverage is computed according to the method outlined in Section 4.2, we can estimate the coverage for this simple case of  $T_1 = 1$  and  $1 - \alpha = 0.50$  using the true model parameter values in (4). From the above discussion, the estimated empirical coverage probability for any  $X_T = x_T$  is given by the maximum value in each row of  $\mathbf{P}$ , namely  $(0.895, 0.500, 0.722, 0.653)$ . Then, in order to obtain a single estimated empirical coverage probability, we need to average those values according to the marginal probability distribution of  $X_T$ , for  $T = 200$ . Again, using the true model (4), the marginal probability distribution is

$$\frac{P(X_T = x_t)}{P(X_T = x_t)} \begin{array}{c|cccc} & x_T = 1 & x_T = 2 & x_T = 3 & x_T = 4 \\ \hline & 0.6206 & 0.0999 & 0.1796 & 0.0999 \end{array}$$

Therefore, we would expect the empirical coverage to be approximately

$$0.895 \cdot 0.6206 + 0.500 \cdot 0.0999 + 0.722 \cdot 0.1796 + 0.653 \cdot 0.0999 = 0.800$$

If we look at the right panel in Figure 2 and find the point associated with  $T_1 = 1$  and  $1 - \alpha = 0.50$ , we see that the point has an empirical coverage probability of approximately 0.800, thus confirming our reasoning for why this likelihood-based approach is over-covering here. In essence, the over-coverage can be explained by the discrete-nature of this problem with a small state-space.

### 4.3 Real Data Analysis

After comparing the CP and likelihood-based prediction approaches on synthetic data in Section 4.2, we apply both prediction algorithms to the real conflict data. We can split this real data analysis into two parts. First, for each country, we use a subset of the observations as calibration data, and then test if the true forecasted state-sequence (defined as the next  $T_1$  time points following the last time point of the calibration data) is within either methods' prediction sets. We then gauge the efficacy of the two prediction algorithms by comparing the empirical coverage averaged across all countries with a prespecified nominal level (i.e., compare reliability curves similar to Figure 2). The second part focuses on constructing prediction sets for a real forecasted state-sequence  $T_1$  time points into the future, beyond the time-frame of the observations in the data. In this case, the calibration data for each country is comprised of *all* observations. While we cannot construct reliability curves for this part, we can get a visual understanding of the forecasted prediction sets using visualizations similar to Figure 3.

For the first part of this analysis, Figure 4 presents the reliability curves for the two prediction methods applied to the real data where the length of the calibration data,  $T$ , is assumed to be all data until December 2024. Similar to Section 4.2, we vary the target coverage  $1 - \alpha \in \{0.50, 0.55, \dots, 1.00\}$  and test length  $T_1 \in \{1, 2, \dots, 6\}$ . For each combination of  $1 - \alpha$  and  $T_1$ , the empirical coverage is computed as follows: for each country, construct the prediction set for the last  $T_1$  time points, determine if that country's true state-sequence is contained within the prediction set, then take the proportion of countries for which the prediction set contains the true sequence. From Figure 4, we see that the

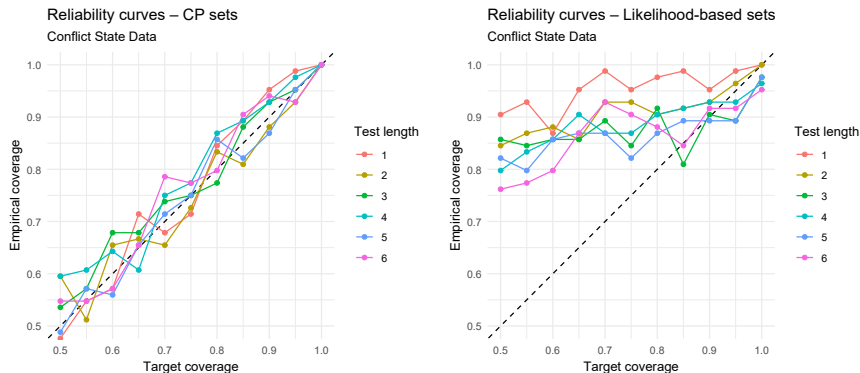


Figure 4: Reliability curves illustrating the relationship between the empirical coverage and the target coverage for both the CP approach (left) and likelihood-based prediction approach (right) for the real conflict data.

application of CP leads to an empirical coverage quite close to the nominal coverage for all  $T_1$ . Contrarily, the likelihood-based approach tends to over-cover for all values of  $T_1$  at lower confidence levels, similar to what is seen in Section 4.2. Additionally, if we focus on the special case of  $1 - \alpha = 1.00$ , we see that for the CP approach, the empirical and target coverages are both equal to one for all  $T_1$ ; however, for the likelihood-based approach, there are values of  $T_1$  such that the empirical coverage is less than one. The justification for this is as follows. In rare cases, the estimated model,  $\hat{\mathbf{P}}$ , will assign zero probability to a state-transition that is possible because that specific state-transition is not observed in the calibration data; henceforth, no state-sequences in the likelihood-based prediction set will contain that specific transition, and so if the true forecasted state-sequence contains that state-transition, it will not be contained in the set, resulting in under-coverage for  $1 - \alpha = 1.00$ . Alternatively, this phenomenon is not observed using CP because  $\hat{\mathbf{P}}$  (from step 2 of Algorithm 1) is computed using the *augmented* state-sequence, not the calibration sequence. This is an important distinction between the CP and likelihood-based predictions, especially if we are interested in forecasting “abnormal” events. The likelihood-based approach can *only* forecast state-sequences consistent with state-transitions observed in the calibration data, whereas the CP approach offers more flexibility and can forecast state-sequences that contain state-transitions unobserved in the calibration sequence.

For the second part of this analysis, we use all of the observed data as the calibration data and construct prediction sets for six months beyond the time horizon of our data ( $T_1 = 6$ ) with a confidence level of  $1 - \alpha = 0.80$ . As an empirical illustration of the method and to highlight the differences with the likelihood-based approach, we focus on four specific countries: Central African Republic, Myanmar, Ethiopia, and Colombia. These countries are selected because they exhibit global diversity, as well as diverse and enduring conflict dynamics, such as prolonged, aborted, and intermittent civil wars that stress-test the forecasting approach across meaningfully different Markovian trajectories.

The results in Figure 5 highlight several important differences between the CP and likelihood-based approaches. While the CP and likelihood-based prediction sets are closely aligned over short forecast horizons, they diverge as the horizon extends. Notably, the likelihood-based sets converge quickly to a stationary distribution, effectively collapsing to a fixed, marginal state distribution as the time horizon increases. The CP sets, by contrast,

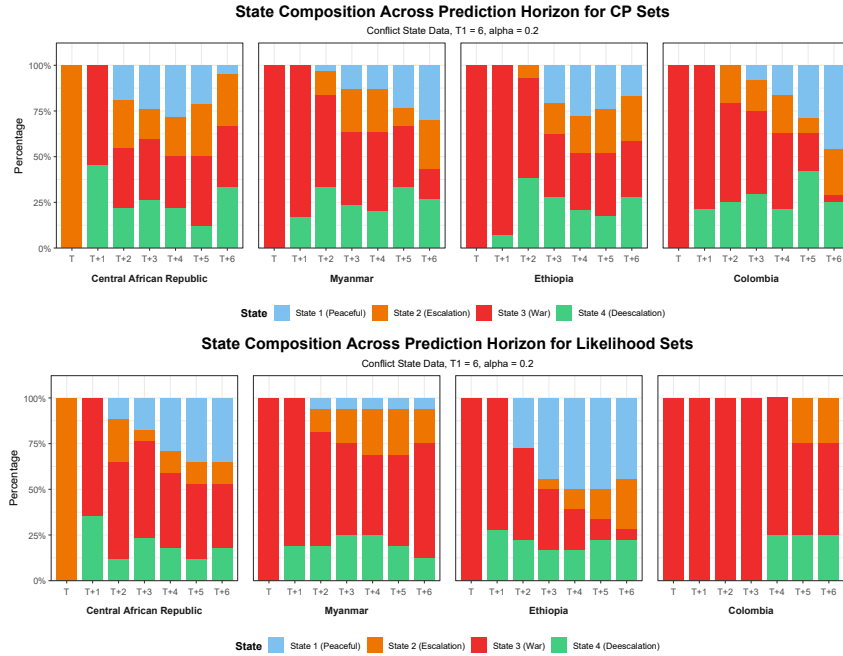


Figure 5: Composition of the prediction sets of forecasted state-sequences using CP (top row) and likelihood-based prediction (bottom row), where  $T_1 = 6$  and  $1 - \alpha = 0.80$ .

retain greater coverage of plausible state-sequences across all forecast steps, reflecting the underlying trajectory uncertainty rather than steady-state behavior. In practical terms, this means CP sets are better positioned to capture the true dynamics of the forecasted sequence when projecting many steps ahead. For short forecast horizons this distinction is minor, but it becomes increasingly consequential when extending beyond the 6-month ( $T_1 = 6$ ) horizon used here toward the 12- or 36-month horizons commonly targeted in the conflict forecasting literature. These patterns exhibited by the likelihood-based approach are visible for all four countries, but are particularly pronounced for Ethiopia and the Central African Republic which have observed conflict at time  $T$  but have relatively low likelihood of observing conflict at time  $T + 6$ . In contrast, the CP sets for these countries include a more diverse set of state-sequences that allow for the possibility of continued conflict at time  $T + 6$ , which is more consistent with the observed conflict dynamics in these countries. In order to see more clearly the convergence of the likelihood-based approach to its stationary distribution, we present in Figure 6 the compositions of both the conformal and likelihood-based prediction sets for  $T_1 = 12$  (i.e., forecasting one year into the future) for specifically Ethiopia and the Central African Republic. Consistent with our reasoning before, the likelihood-based approach exhibits a clear convergent trend whereas the CP approach allows for a wider range of possible states in the later time points. We see stark differences between the two prediction approaches particularly in the expected conflict state at time  $T + 12$ ; the likelihood-based approach indicates a high likelihood of peace in both countries, whereas the CP approach indicates almost the complete reverse (i.e., high chance of conflict). Overall, these results highlight the importance of accounting for model misspecification and uncertainty in transition probabilities when forecasting conflict dynamics, particularly over longer time horizons.

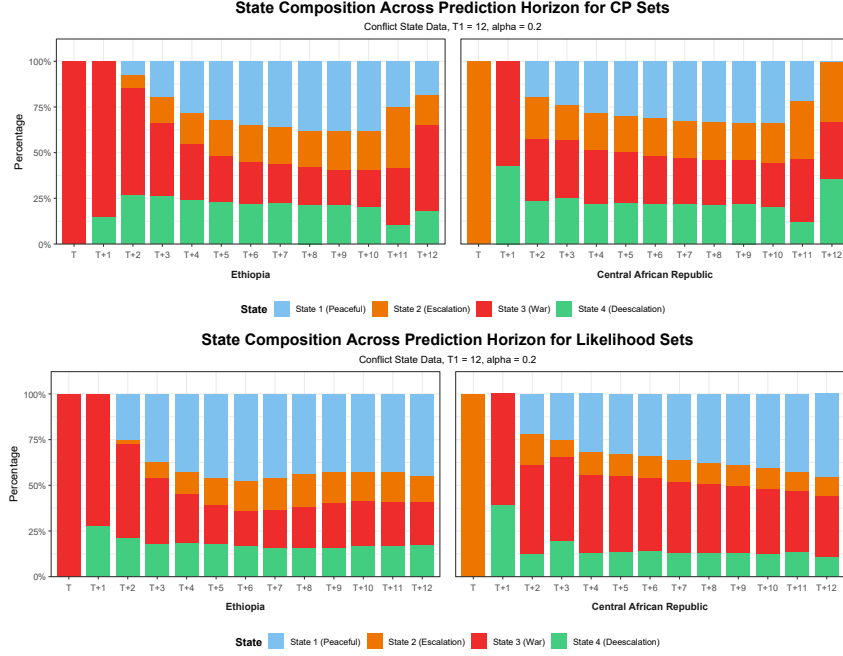


Figure 6: Composition of the prediction sets of forecasted state-sequences, where  $T_1 = 12$  and  $1 - \alpha = 0.80$ .

## 5 Limitations

Recall the data cleaning procedure from Section 4.1. In particular, we exclude countries where a single state perpetuates for the entire duration of the observed time frame. What happens to the results when we *do* include such countries? Consider Sweden, for example, where the country is in peacetime (state 1) for every observation. If we apply Algorithm 1 for  $T_1 = 6$ , Figure 7 illustrates the prediction sets from using both conformal and likelihood-based prediction. Immediately, there is a stark difference between the CP and likelihood-based prediction approaches, moreso than any difference observed in any country in Figure 5. The CP results seem counter-intuitive because in the training/calibration data for Sweden, we have 420 sequential months of state 1 suggesting that the prediction set would have high confidence in predicting a perpetuation of state 1; however, we do not see this. In fact, for  $T = 420$ , the only forecasted state-sequence in the prediction set that ends with  $X_{T+T_1} = 1$  is the state-sequence with  $X_{T+1} = \dots = X_{T+T_1} = 1$ . Thus, why does the CP set contain such a large proportion of forecasted state-sequences that exhibit state-transitions uncharacteristic of the calibration sequence?

Recall that for each possible forecasted state-sequence, the CP algorithm splits the augmented sequence into permutable  $i$ -blocks, and then determines if the proposed forecasted sequence is included in the prediction set by comparing the nonconformity measure of the un-permuted augmented sequence,  $S(\mathbf{I})$ , to the nonconformity measures of all  $i$ -block permutations,  $S(\pi)$  for  $\pi \in \Pi$  (steps 5 and 6 of Algorithm 1). The  $i$ -blocks are completely determined by the state of the last forecasted time point (i.e.,  $i = X_{T+T_1}$ ) and the number of  $i$ -blocks affects the number of possible permutations (i.e.,  $|\Pi|$ ). Figure 8 provides an illustration of how the number of  $i$ -blocks changes depending on the value of  $i = X_{T+T_1}$  in this special case where  $X_1 = \dots = X_T = 1$ . Notice that when  $i = 1$ , each time point in the calibration sequence is an individual  $i$ -block. Therefore, if  $X_{T+1} \neq 1, \dots$ , or  $X_{T+T_1-1} \neq 1$ ,

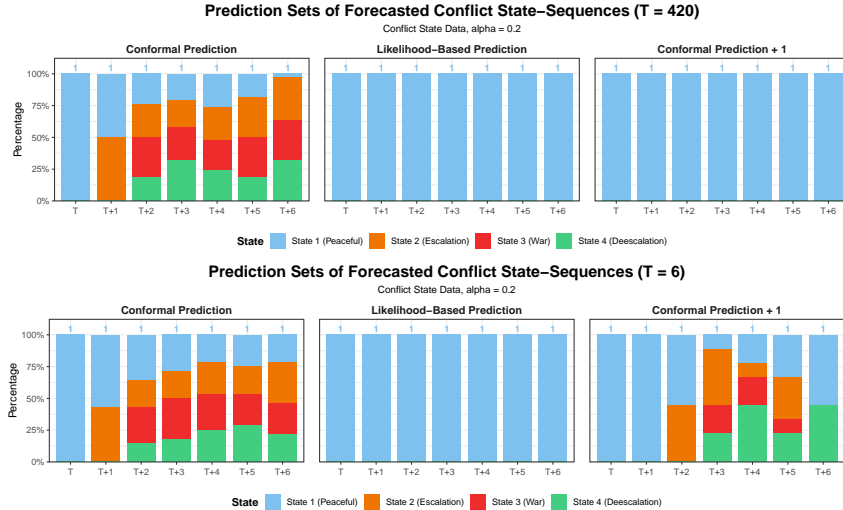


Figure 7: Composition of prediction sets for the special case where all of the calibration data are state 1. These data correspond to Sweden.

$S(\mathbf{I})$  will be large whereas  $S(\pi)$  will be small for almost all  $\pi \in \Pi$ . In other words, when  $X_1 = \dots = X_T = 1$  and  $i = 1$ , the number of  $i$ -blocks (and therefore the number of possible permutations) is large enough to reject the inclusion of state-sequences in the prediction set that are dissimilar to the state-transitions exhibited in the calibration data (i.e., all state 1).

Contrarily, when  $i \in \{2, 3, 4\}$ , the number of  $i$ -blocks dramatically decreases, which has a profound effect on the sequences we accept into the prediction set. Specifically, the entire calibration sequence  $\{X_t\}_{t=1}^T$  is contained within a single non-permutable block,  $I_0$ , as illustrated in Figure 8. Therefore, for each possible forecasted state-sequence  $(x_{T+1}, \dots, x_{T+T_1}) \in \mathcal{X}^{T_1}$  with  $x_{T+T_1} \neq 1$ ,  $S(\mathbf{I})$  and  $S(\pi)$  are no longer so disparate. In these cases, many of the proposed state-sequences are accepted when  $X_{T+T_1} = x_{T+T_1} \neq 1$ . If we consider the special case when  $|\Pi| = 1$  meaning  $S(\mathbf{I}) = S(\pi)$ , we see from step 6 of Algorithm 1 that the proposed state-sequence is accepted as an element of the prediction set with probability  $1 - \alpha$ .

From this discussion, the CP approach is less efficient than the likelihood-based prediction when  $X_1, \dots, X_T$  are all the same state. Note that this is not some arbitrary edge case; in our real data, there exists 105 out of the 191 countries where more than 99% of the observations are state 1 or there exists fewer than five realizations of non-peaceful states (i.e., states 2, 3, or 4). This drawback is certainly an area for future research because ideally, we can construct CP sets that are still valid, but are as efficient as the likelihood-based prediction sets when the calibration data is dominated by a single state. When the last state  $X_{T+T_1}$  matches the dominant state in the calibration data  $\{X_t\}_{t=1}^T$ , we see that the CP approach only includes forecasted sequences that align with the calibration data; however, as soon as the last state differs from the dominant state in the calibration data, the efficiency of the partial exchangeability assumption for CP falls dramatically.

We present a naive solution to this issue by introducing an artificial  $T + T_1 + 1$  time point where  $X_{T+T_1+1} = 1$  always. The third column of Figure 7 presents the resulting CP sets under the title “Conformal Prediction + 1”. We see in the right-most column of Figure 7 with  $T = 420$  that this new CP approach is as efficient as the likelihood-

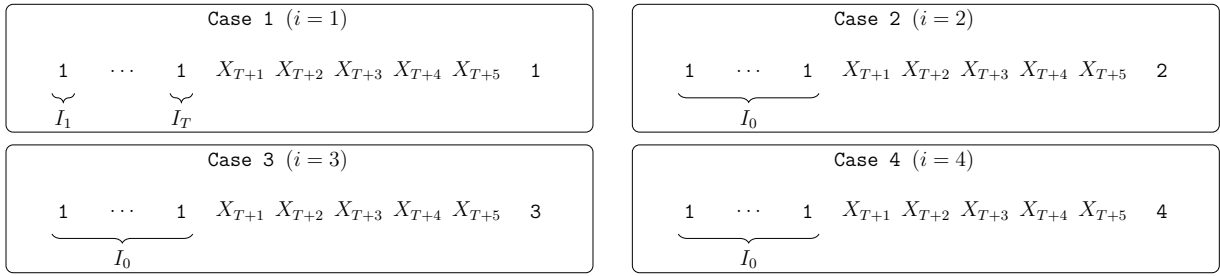


Figure 8: Illustration of how the number of permutable  $i$ -blocks changes depending on the last state, in the special case that all of the training/calibration data are the same state. Note that depending on the realizations for  $(X_{T+1}, \dots, X_{T+5})$ , it is possible for  $I_0$  to extend to further time points (i.e., beyond time  $T$ ) for cases 2, 3, and 4.

based approach where the prediction set contains one state-sequence, namely the sequence  $X_{T+1} = \dots = X_{T+T_1} = 1$ . Then, when  $T = 6$ , this new CP approach produces a prediction set which includes more than one state-sequence (9 sequences to be exact). The reason we say this is a “naive” solution is because our interpretation of the results now slightly differs. Before adding this new  $X_{T+T_1+1} = 1$  time point, we could interpret the prediction sets as the uncertainty quantification for a predicted state-sequence  $T_1$  time points into the future; however, with the additional constraint of  $X_{T+T_1+1} = 1$ , the interpretation of the prediction set now becomes the uncertainty quantification for a predicted state-sequence  $T_1$  time points into the future, *assuming the country returns to peacetime at time  $T + T_1 + 1$* . We leave this issue as future work, but highlight it as an important limitation that was not discussed/addressed in Nettasinghe et al. [2023].

## 6 Conclusion

Forecasting the conflict dynamics for a given country many months into the future has influence over a country’s geopolitics. While a single point-prediction of a conflict state-sequence is easily interpretable, of tantamount importance is how certain that prediction is. Therefore, we present an application of CP for Markov processes in constructing prediction sets that are finite-sample valid for any prespecified confidence level. The utility of using this machine learning architecture is its robustness to model misspecification. Beyond achieving appropriate nominal coverage rates, a key advantage of the CP approach over likelihood-based simulation becomes increasingly apparent as the forecast horizon extends. Likelihood-based prediction sets may converge to a stationary distribution (collapsing to fixed state probabilities), thereby losing the ability to reflect genuine trajectory uncertainty. CP sets, by contrast, retain coverage of plausible state-sequences across all forecasted steps, preserving the temporal dynamics that are of substantive interest in many applications.

For the purposes of this article, no covariate information is used in either prediction algorithms. That said, both the CP and likelihood-based prediction strategies naturally extend to the scenario where the transition probabilities between states depend on covariates. We leave this to future work.

## References

- Håvard Hegre, Marie Allansson, Matthias Basedau, Michael Colaresi, Mihai Croicu, Hanne Fjelde, Frederick Hoyles, Lisa Hultman, Stina Höglbladh, Remco Jansen, et al. Views: A political violence early-warning system. *Journal of peace research*, 56(2):155–174, 2019.
- Håvard Hegre, Curtis Bell, Michael Colaresi, Mihai Croicu, Frederick Hoyles, Remco Jansen, Maxine Ria Leis, Angelica Lindqvist-McGowan, David Randahl, Espen Geelmuyden Rød, et al. Views2020: revising and evaluating the views political violence early-warning system. *Journal of peace research*, 58(3):599–611, 2021.
- David Randahl, Maxine Leis, Tim Gåsste, Hanne Fjelde, Håvard Hegre, Staffan I Lindberg, and Steven Wilson. Forecasting electoral violence. *International journal of forecasting*, 2025.
- Michael D Ward and Andreas Beger. Lessons from near real-time forecasting of irregular leadership changes. *Journal of Peace Research*, 54(2):141–156, 2017.
- Richard Morgan, Andreas Beger, and Adam Glynn. Varieties of forecasts: Predicting adverse regime transitions. *V-Dem Working Paper*, 89, 2019.
- Håvard Hegre, Paola Vesco, Michael Colaresi, Jonas Vestby, Alexa Timlick, Noorain Syed Kazmi, Angelica Lindqvist-McGowan, Friederike Becker, Marco Binetti, Tobias Bodentien, et al. The 2023/24 views prediction challenge: Predicting the number of fatalities in armed conflict, with uncertainty. *Journal of Peace Research*, 62(6):2070–2087, 2025.
- David Randahl, Jonathan P Williams, and Håvard Hegre. Bin-conditional conformal prediction of fatalities from armed conflict. *Political Analysis*, 34(1):96–108, 2026.
- David Randahl and Johan Vegelius. Predicting escalating and de-escalating violence in africa using markov models. *International Interactions*, 48(4):597–613, 2022.
- Jonathan P Williams, Gudmund H Hermansen, Håvard Strand, Govinda Clayton, and Håvard Mogleiv Nygård. Bayesian hidden markov models for latent variable labeling assignments in conflict research: Application to the role ceasefires play in conflict dynamics. *Annals of Applied Statistics*, 18(3):2034–2061, 2024.
- David Randahl and Johan Vegelius. Forecasting densities of fatalities from state-based conflicts using observed markov models. *arXiv preprint arXiv:2410.12374*, 2024.
- Glenn Shafer and Vladimir Vovk. A tutorial on conformal prediction. *Journal of Machine Learning Research*, 9(3), 2008.
- Vladimir Vovk, Alexander Gammerman, and Glenn Shafer. *Algorithmic Learning in a Random World*. Springer International Publishing, 2 edition, 2022. ISBN 9783031066481. doi: 10.1007/978-3-031-06649-8.
- Anders Hjort, Jonathan P Williams, and Johan Pensar. Clustered conformal prediction for the housing market. *Proceedings of Machine Learning Research*, 230:1–21, 2024.

- Anders Hjort, Gudmund Horn Hermansen, Johan Pensar, and Jonathan P Williams. Uncertainty quantification in automated valuation models with spatially weighted conformal prediction. *International Journal of Data Science and Analytics*, 20(8):7089–7106, 2025.
- Heeseung Bang, Aditya Dave, and Andreas A Malikopoulos. Safe merging in mixed traffic with confidence. *arXiv preprint arXiv:2403.05742*, 2024.
- Huiying Mao, Ryan Martin, and Brian J Reich. Valid model-free spatial prediction. *Journal of the American Statistical Association*, 119(546):904–914, 2024.
- Mikhail Dashevskiy and Zhiyuan Luo. Network traffic demand prediction with confidence. In *IEEE GLOBECOM 2008-2008 IEEE Global Telecommunications Conference*, pages 1–5. IEEE, 2008.
- Rui Luo, Buddhika Nettasinghe, and Vikram Krishnamurthy. Anomalous edge detection in edge exchangeable social network models. In *Conformal and probabilistic prediction with applications*, pages 287–310. PMLR, 2023.
- Chen Xu and Yao Xie. Conformal prediction interval for dynamic time-series. In *International Conference on Machine Learning*, pages 11559–11569. PMLR, 2021.
- Chen Xu and Yao Xie. Conformal prediction for time series. *IEEE transactions on pattern analysis and machine intelligence*, 45(10):11575–11587, 2023.
- Frédéric Zheng and Alexandre Proutiere. Conformal predictions under markovian data. *arXiv preprint arXiv:2407.15277*, 2024.
- Sonakshi Dua, Gonzalo Mateos, and Sundeep Prabhakar Chepuri. Conformal inference for time series over graphs. *arXiv preprint arXiv:2510.11049*, 2025.
- Roberto Neglia, Andrea Cini, Michael M Bronstein, and Filippo Maria Bianchi. Rescp: Reservoir conformal prediction for time series forecasting. *arXiv preprint arXiv:2510.05060*, 2025.
- Isaac Gibbs and Emmanuel Candes. Adaptive conformal inference under distribution shift. *Advances in Neural Information Processing Systems*, 34:1660–1672, 2021.
- Margaux Zaffran, Olivier Féron, Yannig Goude, Julie Josse, and Aymeric Dieuleveut. Adaptive conformal predictions for time series. In *International Conference on Machine Learning*, pages 25834–25866. PMLR, 2022.
- Xiaoyi Su, Zhixin Zhou, and Rui Luo. Adaptive conformal inference by particle filtering under hidden markov models. *arXiv preprint arXiv:2411.01558*, 2024.
- Giovanni Cherubin and Ilia Nourtdinov. Hidden markov models with confidence. In Alexander Gammerman, Zhiyuan Luo, Jesús Vega, and Vladimir Vovk, editors, *Conformal and Probabilistic Prediction with Applications*, pages 128–144, Cham, 2016. Springer International Publishing. ISBN 978-3-319-33395-3.
- Kamile Stankeviciute, Ahmed M Alaa, and Mihaela Van der Schaar. Conformal time-series forecasting. *Advances in neural information processing systems*, 34:6216–6228, 2021.

Victor Chernozhukov, Kaspar Wüthrich, and Zhu Yinchu. Exact and robust conformal inference methods for predictive machine learning with dependent data. In *Conference On learning theory*, pages 732–749. PMLR, 2018.

Victor Chernozhukov, Kaspar Wüthrich, and Yinchu Zhu. An exact and robust conformal inference method for counterfactual and synthetic controls. *Journal of the American Statistical Association*, 116(536):1849–1864, 2021.

Buddhika Nettasinghe, Samrat Chatterjee, Ramakrishna Tipireddy, and Mahantesh M Halappanavar. Extending conformal prediction to hidden Markov models with exact validity via de Finetti’s theorem for Markov chains. In *International conference on machine learning*, pages 25890–25903. PMLR, 2023.

Shawn Davies, Therése Pettersson, Margareta Sollenberg, and Magnus Öberg. Organized violence 1989–2024, and the challenges of identifying civilian victims. *Journal of Peace Research*, 62(4):1223–1240, 2025.

Ralph Sundberg and Erik Melander. Introducing the ucdp georeferenced event dataset. *Journal of peace research*, 50(4):523–532, 2013.

## 7 Appendix: Alternative Likelihood-Based Prediction Strategies

The likelihood-based prediction set defined in (3) minimizes the cardinality of the  $(1 - \alpha)$ -level prediction sets ( $\alpha \in [0, 1]$ ), and guarantees that *each*  $\mathcal{C}_{1-\alpha}^{\text{like}}$  obtains a cumulative probability mass of at least  $1 - \alpha$ . However, as shown in Figures 2 and 4, the empirical coverage from this likelihood-based approach tends to exceed, on average, the desired coverage level. As a result, we present an alternative likelihood-based prediction strategy that results in better calibrated coverage, on average, at the sacrifice of *not* guaranteeing each prediction set obtains cumulative probability mass of at least  $1 - \alpha$ .

Let  $\mathcal{C}_{1-\alpha}^{\text{like}^*}$  denote this alternative likelihood-based prediction set for desired coverage level  $1 - \alpha$ . We follow all of the steps in Section 3.2 leading up to the construction of the prediction set; however, now the prediction set is defined as

$$\mathcal{C}_{1-\alpha}^{\text{like}^*} := \{\mathbf{x}^{(1)}, \dots, \mathbf{x}^{(K)}\} \cdot \mathbf{1}\{u^* \leq p\} + \{\mathbf{x}^{(1)}, \dots, \mathbf{x}^{(K-1)}\} \cdot \mathbf{1}\{u^* > p\},$$

where  $u^*$  is a realization of  $U^* \sim \text{Uniform}[0, 1]$ , and

$$p = \begin{cases} \frac{1 - \alpha}{\mathbb{P}(\mathbf{X}_{T+1}^{T+T_1} = \mathbf{x}^{(K)} \mid X_T = x_T)}, & K = 1 \\ \frac{(1 - \alpha) - \sum_{j=1}^{K-1} \mathbb{P}(\mathbf{X}_{T+1}^{T+T_1} = \mathbf{x}^{(j)} \mid X_T = x_T)}{\mathbb{P}(\mathbf{X}_{T+1}^{T+T_1} = \mathbf{x}^{(K)} \mid X_T = x_T)}, & K > 1. \end{cases}$$

This choice of  $p$  guarantees that the *expected* cumulative probability mass from  $\mathcal{C}_{1-\alpha}^{\text{like}^*}$  will equal  $1 - \alpha$ . More formally, for  $K > 1$ ,

$$\begin{aligned}
& \mathbb{E} \left\{ \left[ \sum_{j=1}^K \mathbb{P}(\mathbf{X}_{T+1}^{T+T_1} = \mathbf{x}^{(j)} \mid X_T = x_T) \right] \cdot \mathbf{1}\{U^* \leq p\} + \left[ \sum_{j=1}^{K-1} \mathbb{P}(\mathbf{X}_{T+1}^{T+T_1} = \mathbf{x}^{(j)} \mid X_T = x_T) \right] \cdot \mathbf{1}\{U^* > p\} \right\} \\
&= \left[ \sum_{j=1}^K \mathbb{P}(\mathbf{X}_{T+1}^{T+T_1} = \mathbf{x}^{(j)} \mid X_T = x_T) \right] \cdot \mathbb{P}\{U^* \leq p\} + \left[ \sum_{j=1}^{K-1} \mathbb{P}(\mathbf{X}_{T+1}^{T+T_1} = \mathbf{x}^{(j)} \mid X_T = x_T) \right] \cdot \mathbb{P}\{U^* > p\} \\
&= \left[ \sum_{j=1}^K \mathbb{P}(\mathbf{X}_{T+1}^{T+T_1} = \mathbf{x}^{(j)} \mid X_T = x_T) \right] \cdot p + \left[ \sum_{j=1}^{K-1} \mathbb{P}(\mathbf{X}_{T+1}^{T+T_1} = \mathbf{x}^{(j)} \mid X_T = x_T) \right] \cdot (1-p) \\
&= p \cdot \mathbb{P}(\mathbf{X}_{T+1}^{T+T_1} = \mathbf{x}^{(K)} \mid X_T = x_T) + \sum_{j=1}^{K-1} \mathbb{P}(\mathbf{X}_{T+1}^{T+T_1} = \mathbf{x}^{(j)} \mid X_T = x_T) \\
&= (1-\alpha) - \sum_{j=1}^{K-1} \mathbb{P}(\mathbf{X}_{T+1}^{T+T_1} = \mathbf{x}^{(j)} \mid X_T = x_T) + \sum_{j=1}^{K-1} \mathbb{P}(\mathbf{X}_{T+1}^{T+T_1} = \mathbf{x}^{(j)} \mid X_T = x_T) \\
&= 1 - \alpha.
\end{aligned}$$

The reason we ultimately elect *not* to implement this in the manuscript is because, again, it no longer guarantees that  $\mathcal{C}_{1-\alpha}^{\text{like}^*}$  is a  $1 - \alpha$  probability set with respect to the probability distribution over the space of sequences. Of course, on average it will be calibrated to  $1 - \alpha$  coverage, but its interpretation may appear as suspicious to practitioners. To illustrate, the following is also a perfectly calibrated  $1 - \alpha$  level prediction set:

$$\mathcal{X}^{T_1} \cdot \mathbf{1}\{u^* \leq 1 - \alpha\} + \emptyset \cdot \mathbf{1}\{u^* > 1 - \alpha\},$$

i.e., the set that is either the entire set of possible forecasted state-sequences ( $\mathcal{X}^{T_1}$  with  $\mathbb{P}(\mathcal{X}^{T_1}) = 1$ ) or the empty-set ( $\emptyset$  with  $\mathbb{P}(\emptyset) = 0$ ).